Mem. S.A.It. Vol. 81, 69

Memorie della

Suzaku view of soft X-ray diffuse background in 0.4 - 1 keV

K. Mitsuda[1], T. Yoshino[1], N.Y. Yamasaki[1], Y. Takei[1], T. Hagihara[1], K. Masui[1], M. Bauer[1,2], D. McCammon[3], R. Fujimoto[4], Q.D. Wang[5], and Y. Yao[6,7]

[1] Institute of Space and Astronautical Science, Japan Aerospace Exploration Agency, 3-1-1 Yoshinodai, Sagamihara, 229-8510, Japan
[2] Max-Planck-Institut für extraterrestrische Physik, 85748 Garching, Germany
[3] Department of Physics, University of Wisconsin, Madison, 1150 University Avenue, Madison, WI 53706, USA
[4] Department of Physics, Kanazawa University, Kanazawa, 920-1192, Japan
[5] Department of Astronomy, University of Massachusetts Amherst, MA 01003, USA
[6] Massachusetts Institute of Technology (MIT) Kavli Institute for Astrophysics and Space Research, 70 Vassar Street, Cambridge, MA 02139, USA
[7] University of Colorado, CASA, 389 UCB, Boulder, CO 80309, USA

Abstract. The origins of the soft diffuse X-ray background are discussed basing on recent Suzaku observations. The O VII and O VIII intensities of fourteen different fields were determined with Suzaku with relatively small statistical and systematic errors. The O VII and O VIII intensities show strong correlations: O VII emission shows an intensity floor at $\sim$ 2 photons s^{-1} cm^{-2} str^{-1} (LU), while the high-latitude O VIII emission shows a tight correlation with excess of O VII emission above the floor, with (O VIII intensity) = 0.5 $\times$ [(O VII intensity) – 2 LU], suggesting that temperatures averaged over different line-of-sight show a narrow distribution around $\sim$ 0.2 keV. We consider that the offset intensity of O VII arises from the Heliospheric solar wind charge exchange, and that the excess O VII (2-7 LU) is emission from more distant parts of the Galaxy, which may be regarded as the halo of our Galaxy. The total bolometric luminosity of this galactic emission is estimated to be 4×10^{39} erg s^{-1}, and its characteristic temperature may be related to the virial temperature of the Galaxy.

Key words. Galaxy: disk — Galaxy: halo — X-rays: diffuse background — X-rays: ISM

1. Introduction

The X-ray sky below 1 keV is quite uniform after subtracting individual sources and local diffuse emission such as the north polar spur, and galactic bulge (Figure 1). The emission is often called the soft X-ray diffuse background (SXDB) and is considered to arise from faint extragalactic sources and emissions from highly ionized ions, such as C VI, O VII, O VIII, Fe XVII, and Ne IX, in solar neighborhoods and in our Galaxy. The extragalactic contribution, which we refer to as the Cosmic X-ray Background (CXB) in this paper, is estimated to be about 40 % of emission in the ROSAT

Send offprint requests to: K. Mitsuda

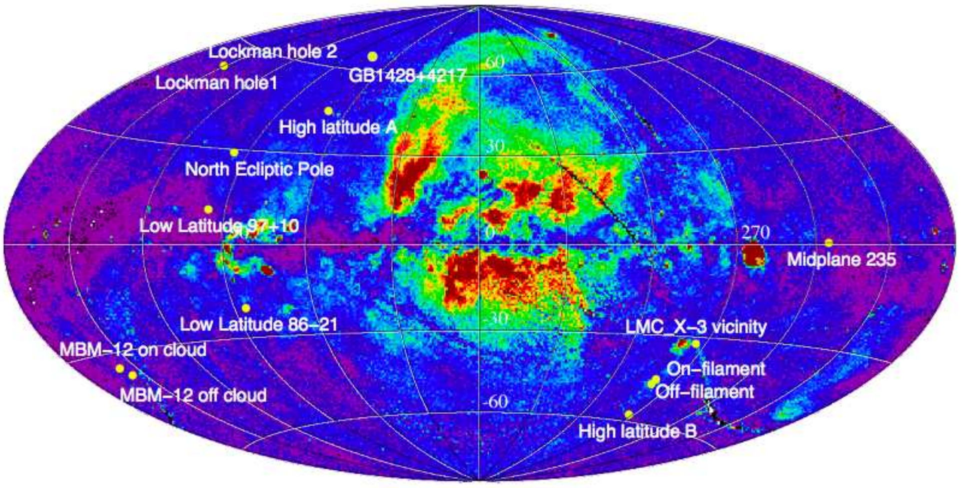

Fig. 1. ROSAT diffuse X-ray R45 band map (Snowden et al. 1997), and the directions of fourteen fields in this paper.

R45 band (McCammon et al. 2002), which is approximately $\sim 0.44 - 1$ keV. The emission from highly ionized ions is considered to arise from at least three different origins; the solar wind charge exchange (SWCX) induced emission from the Heliosphere (Cox 1998; Cravens 2000; Lallement 2004), the thermal emission from the hot gas in local hot bubble (LHB) (McCammon & Sanders 1990), and emission from more distant part of the galaxy, mostly above or beyond the bulk of absorption in the Galactic disk. It is hard to separated the first two emission component from each other using emission spectra above ~ 0.4 keV. Moreover, there are accumulating observational evidences that above ~ 0.4 keV the contribution of the LHB is small compared to that of the Heliospheric SWCX(e.g. Smith et al. (2007)). In this energy range, the sum of the two emission components are often approximated by a thin-thermal emission of kT $\sim$ 0.1 keV without absorption (Smith et al. 2007; Henley et al. 2007; Galeazzi et al. 2007; Kuntz & Snowden 2008; Masui et al. 2009), although there is no strong reason that the Heliospheric SWCX can be apporximated by a single thermal emission. Kuntz & Snowden (2000) called the third component the "transabsorption" emission (TAE) and separated it in the ROSAT all sky map utilizing the directional dependence of the absorption column density. They found that the emission spectrum can be described by a two-temperature thermal emission model of temperatures kT $\sim$ 0.10 and 0.25 keV. However, because there is no constraint on distance other than absorption, it is hard to constrain the origins conclusively.

In this paper we review recent Suzaku (Mitsuda et al. 2007) observations performed according to two different strategies to constrain the origins of the SXDB. By virtue of the good energy spread function of the CCD camera (Koyama et al. 2007) and the high sensitivity to spatially diffuse emission when combined with the X-ray mirror (Serlemitsos et al. 2007), we can determined intensities of O VII and O VIII emission with small systematic errors. We will find that correlations of O VII and O VIII intensities determined for the fourteen fields strongly suggest two different origins of emission (Yoshino et al. 2009). The high resolution spectroscopy using the transmission gratings onboard Chandra enables detailed study of absorption lines in bright X-ray sources. O VII and O VIII absorption lines of some sources are considered to arise from highly ionized ions which are responsible for the SXDB. We observed vicinities of LMC X-3 from which absorption lines were detected. The combined analysis of emission and absorption spectra will constrain the density and spatial extent simultaneously (Yao et al. 2009).

2. Spectra of fourteen fields

Fujimoto et al. (2007) reported a flare-like increase of X-ray flux during the Suzaku observation of the North Ecliptic Pole in September 2005 (NEP1). The increased component of spectrum mostly consists of emission lines from highly ionized ions. The increase in O VII intensity was ~ 5photons s^{-1} cm^{-2} str^{-1} (LU). Thus is comparable or even larger than the O VII Intensity in the SXDB. Such short (< 1 day) term time variation is most likely from interaction with highly ionized ions and neutrals in Earth's geocorona (e.g. Cravens et al. (2001)). The flare in the Suzaku NEP1 observation was clearly visible in the light curve of 256 s time bins. However, in most cases time variations are not visible with in light curves because of insufficient photon statistics. The contamination is sometimes still significant when the spectrum is integrated for a few 10 ks or more. An example is shown in Figure 2.

In order to to find the contamination, we sorted the data according to two parameters, the solar-wind proton flux at the Earth and the the Earth-center to magnetopause (ETM) distance, where the magnetopause is defined as the lowest position along the sight line of Suzaku where geomagnetic field is open to interplanetary space. Since Suzaku is in a low earth orbit of an about 570 km altitude, it always looks at the sky through the magnetopause. Solar-wind ions may penetrate down to the ETM distance and the density of neutral proton in the geocorona is higher with lower ETM distance. Thus the probability of a contamination in Suzaku spectra by the SWCX from the geocorona increases if the shortest Earth-center to magnetopause (ETM) distance is $\lesssim 5\ R_{\rm E}$ (Fujimoto et al. 2007). When we find more than 2 σ difference in the O VII intensity among the subset of data with different proton flux or the ETM distance, we discard the high O VII flux subset. Please see Yoshino et al. (2009) for more details of the procedure.

2.1. Correlation between O VII and O VIII intensities and two different origins

In Figure 3, we plot the derived O VIII emission intensity of the fourteen fields as a function of the O VII intensity. In the figure we notice two remarkable characteristics. First, there is a floor in the O VII intensity at ~ 2 LU. Second, all the data points except for three approximately follow the relation (O VIII intensity) = 0.5 × [(O VII intensity) - 2 LU]. Threre are five fields are on the O VII intensity floor. Three of them, Midplane 235 (denoted as MP235 in Figure 3), $(\ell, b) = (235.0, 0.0)$), Low lattitude 97+10 (LL10, (96.6, 10.4)), and MBM-12 on cloud (M12on, (159.2, -34.5)), have a large absorption column densities of $(3-9)\times10^{21}\mathrm{cm}^{-2}$. Masui et al. (2009) proposed that the O VIII emission line of the midplane field, MP235, is associated with a ~ 0.8 keV component that may arise from faint young dM stars in the Galactic disk. Another low-attitude field at $b = 10°$, LL10, is also considered to contain emission of similar origin. Such high temperature emission produces little O VII. Assuming the midplane space-averaged neutral density (Ferrière 2001), the absorption length of O VII emission is estimated to be 300 pc for MP235. The total Galactic absorption column density of LL10 ($|b| = 10°$) is $2.7 \times 10^{21}\mathrm{cm}^{-2}$, through which only 10 % of O VII photons can penetrate. The M12on field is towards the molecular cloud MBM-12. O VII emission must arise from the near side of the MBM-12 molecular cloud whose distance is 60 - 300 pc. These indicate that the floor component is "local" emission, i.e. the emission must arise with in ~ 300 pc from the Earth.

A part of emission in the ROSAT R12 band (0.15-0.28 keV) is considered to arise from the LHB, because it shows anti-correlations

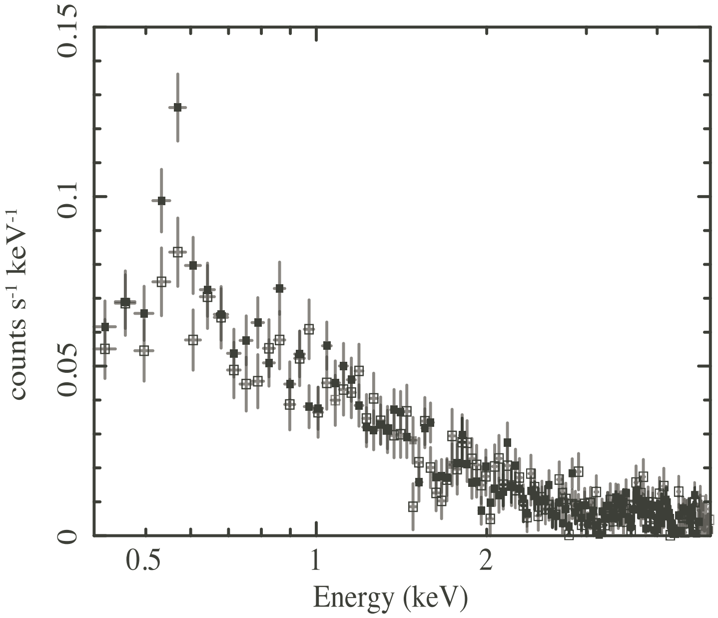

Fig. 2. Energy spectra of High Latitude B (HL-B) for the time intervals with solar wind proton flux higher (filled squares) or lower (open squares) than 4×10^8 protons s^{-1} cm^{-2}. The vertical error bars are the $1 - \sigma$ statistical errors. The non X-ray background was subtracted. There are large ($> 3\ \sigma$) discrepancies between the O VII emission ($\sim$ 0.56 keV) intensities of two spectra, which indicates significant geocoronal SWCX contamination in the higher proton-flux data.

with the N_H of the direction, which is interpreted by the displacement model. On the other hand, recent observational results indicates that the LHB contribute to the emission in the ROSAT R45 band only a little ($\lesssim 1/20$, see discussion in Smith et al. (2007)). During solar minimum, the solar wind has a rather simple structure, with the slow wind confined to low ecliptic latitudes ($|E_{lat}| \lesssim 20°$). However the spatially non-uniform distribution of neutral H and He around the Sun leads to a complex pattern of Heliospheric SWCX emissivity. Moreover, the observed SWCX emission intensity is also a function of the observer's particular viewing geometry, as noted for example by Lallement (2004) and Robertson & Cravens (2003). According to the simulation by Koutroumpa et al. (2006), near the solar minimum, the amplitude of the spatial intensity variation of O VII intensity is within the systematic errors of the O VII intensity due to uncertainty in the removal of Geocoronal SWCX ($\sim$ 1.5 LU, see Yoshino et al. (2009)) for $|E_{lat}| \gtrsim 20°$. The average intensity is $\sim$ 1.5 LU. The twelve fields are happen to be in $|E_{lat}| \gtrsim 38°$. Thus the floor intensity is consistent with the Heliospheric SWCX.

The linear component is likely to arise from more distant part of our Galaxy. It is remarkable that the field with (86.0, -20.8) contains significant linear component (6.4 - 2 = 4.4 LU), even though the low Galactic latitude. The absorption column density of this direction, 7.2×10^{20} cm^{-2}, is about quarter of that of the field on the floor, LL10 and the transmission of the O VII emission is about 54 %. This suggests that a large fraction of the linear component arises from beyond the bulk of Galactic absorption, although the possibility that the difference between LL10 and LL21 is mainly due to spatial fluctuation of the emission measure cannot be ruled out. We thus consider that the linear component is associated with the TAE component, which may be regarded

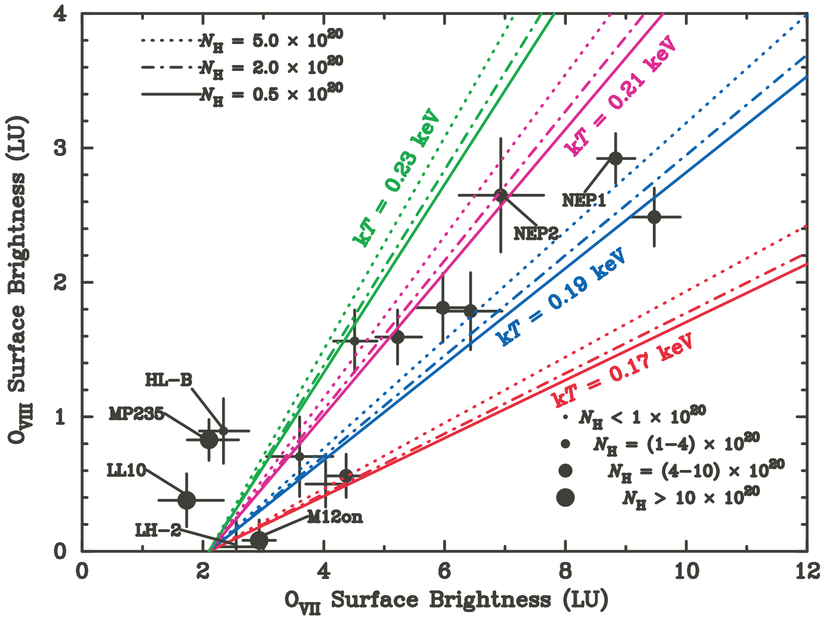

Fig. 3. Relation between O VII and O VIII surface brightnesses for the 14 sky fields observed with Suzaku. The horizontal and vertical bars of data points show the 1 σ errors of the estimation. The contribution of O VII K_β emission in the Gaussian function for O VIII K_α is subtracted. The diagonal lines show the relation between O VII and O VIII, assuming an offset O VII emission of 2.1 LU and emission from a hot plasma of the temperature and the absorption column density shown in the figure. The Galactic absorption column density of the observation fields are indicated by the maker size of the data points. The short names of five data points on the intensity floor of O VII emission are also shown.

as emission from the halo of our Galaxy. This component emits O VII and O VIII with an intensity ratio of about 2 to 1 and shows field-to-field variations of ∼ 0 to ∼ 7 LU in O VII intensity.

The lines in Figure 3 show O VII - O VIII intensity relations for different temperatures and absorption column densities. We have assumed 2.1 LU as the O VII floor intensity, using the value for the midplane field (MP235). The lines suggest that the average temperatures along each line of sight of the plasmas emitting the O VIII emission and the O VII emission above the floor are in a relatively narrow range of kT ∼ 0.19 to 0.23 keV if they are arising from collisionally equilibrium plasma in spite of the large O VII intensity variations (∼ 0 to ∼ 7 LU).

3. Spatial distribution and the origin of the TAE component

An emission intensity of a line is proportional to the emission measure which is proportional to $n_{\rm ion}^2 L$, while an equivalent width of an absorption line is proportional to the column density, $n_{\rm ion}L$. Thus it is possible to constrain $n_{\rm ion}$ and L independently if we observe an absorption line and an emission line from a same ion of a same plasma. Yao et al. (2009) reported a combined analysis of absorption spectra of LMC X-3, the X-ray binary in the LMC, observed with Chandra and emission spectra vicinity of (∼ 30′) LMC X-3 obtained with Suzaku. Hagiharar et al. (2009) recently reported results of similar analysis for PKS 2155-304.

Yao et al. (2009) constructed a thick hot disk model extending above the Galactic disk

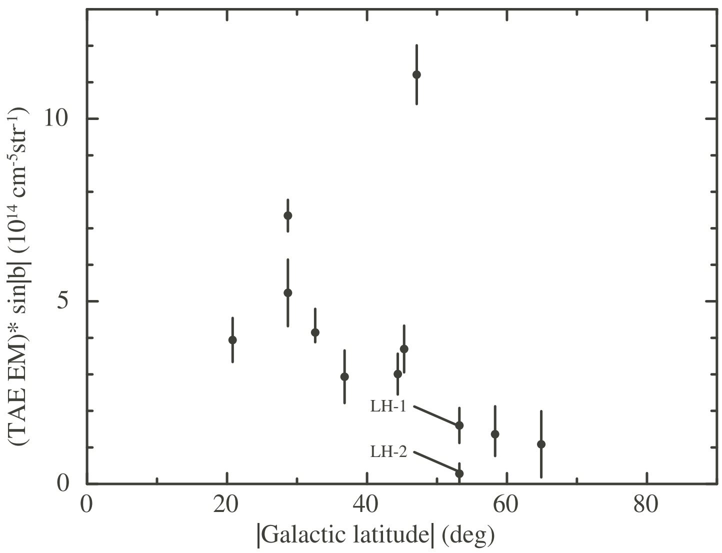

Fig. 4. The emission measure of the TAE component multiplied by sin $|b|$ as a function of $|b|$.

in order to simultaneously explain the absorption and emission lines. They assumed density and temperature distributions exponentially decreasing in the direction perpendicular to the Galactic disk. They obtained as the best-fit parameters the scale heights of $h_T\xi = 1.4(0.2, 5.2)$ kpc and $h_n\xi = 2.8(1.0, 6.4)$ kpc for temperature and density respectively, and the midplane gas temperature and H ion density of $T_0 = 3.6(2.9, 4.7) \times 10^6$ K and $n_0 = 1.4(0.3, 3.4) \times 10^{-3}\text{cm}^{-3}$, where ξ is the filling factor of the hot gas. The emission-measure weighted average temperature along a line of sight is $T_0/(1 + h_n/(2h_T)) \sim 0.16$ keV. This is lower than the best-fit temperatures of the TAE component, although the discrepancy is not very large taking the the errors in T_0 and h_n/h_T into account.

For a plane-parallel configuration, we expect the intensity of the emission to increase from high to low latitude as $\propto \sin^{-1}|b|$,with a rapid decrease at low latitudes, $b \lesssim 10°$, due to Galactic absorption with a much smaller scale height than the emission. In Figure 4, instead of O VII emission intensity, we show the emission measure of the TAE component obtained from the spectral fits multiplied by sin $|b|$ (EM sin $|b|$). EM sin $|b|$ shows a tendency to decrease with increasing $|b|$ and at the same time a direction-to-direction fluctuation. This may suggest that the hot gas is more extended in outer rim of the Galaxy and that the hot gas is patchy and consists of number of blobs.

Yao et al. (2009) concluded that the plasma responsible for the O VII and O VIII absorption and emission towards LMC X-3 cannot be isothermal. However, the temperatures averaged over line of sight for various directions determined by O VII to O VIII ratio was remarkably constant (Figure 3). The radiative cooling time of the hot gas is 3 Gy, thus the hot gas needs be supplied at least on this time scale. A possible origin of the hot gas is supernovae. In fact both the total mass and the total thermal energy of the hot plasma can be supplied at a supernova rate of 10^{-2} y^{-1} within the radiative cooling time.

However, there is no particular reason why the gas should prefer $kT = 0.2$ keV. The spectra of the halo emission of nearby star-forming galaxies and of some of normal galaxies are described by two-temperature models with kT's in the range of 0.1 to 0.8 keV (Strickland et al. 2004; Tüllman et al. 2006;

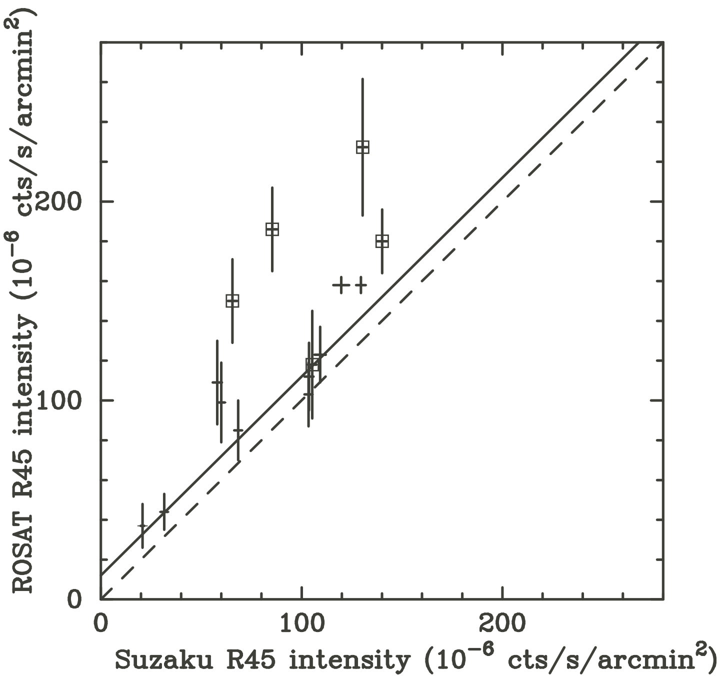

Fig. 5. Observed ROSAT R45 band counting rate v.s. counting rate expected from Suzaku best-fit model functions. Points with open boxes are from regions in the ROSAT survey which are possibly contaminated by the geocoronal SWCX or scattering of solar X-ray. The vertical error bars are the 1 σ statistical errors of the ROSAT observation. The horizontal error bars are 1 σ statistical errors estimated from the spectral model fits of Suzaku data. The diagonal solid line shows the predicted relation corrected for the difference in point source removal levels of two missions.

Yamasaki et al. 2009). Thus we consider that $kT = 0.2$ keV is specific for our Galaxy. Then it is likely related to the virial temperature ($kT = 0.2$ keV) for the rotation velocity of 200 km s^{-1} (e.g. Kereš et al. (2005)). A possible scenario may be that higher temperature gas has escaped from the potential and that the gas at the temperature near the virial temperature remains, since the escape time scale is by a factor of five shorter than the radiative cooling time scale.

We estimate the parameters of hot gas by assuming an isotropic temperature of $kT = 0.222$ keV for simplicity. The total luminosity of the emission is estimated from the average value of $EM \sin|b|$, assuming a plane parallel density distribution as

$$L = 8\pi^2 \Lambda(T) \overline{EM \sin|b|} R^2,$$

where $\Lambda(T)$ and R are, respectively, the emissivity per emission measure at a temperature T, and the outer cylindrical radius of the emission region. Using the values of $\Lambda(T)$ for bolometric flux (Sutherland & Dopita 1993) and 0.3-2 keV band (APEC), we obtain, $L_{\rm bol} = 3.8 \times 10^{39}$ erg s^{-1} and $L_{0.3-2\rm keV} = 1.1 \times 10^{39}$ erg s^{-1} for $\overline{EM \sin|b|} = 3.6 \times 10^{14}$ cm^{-5} str^{-1} and $R = 15$ kpc. The midplane density and the total mass of the hot gas, $M_{\rm tot}$, can be estimated by further assuming the scale height. $n_0 = 1.3 \times 10^{-3}$ cm^{-3} and $M_{\rm tot} = 6.5 \times 10^7 M_\odot$ with $h\xi = 1.4$kpc.

4. DISCUSSION

Matteo GUAINAZZI: Have you compared the floor component of the SWCX with measurements by XMM-Newton?

There are several papers in which the O VII and O VII intensities obtained with Suzaku were compared with those of XMM-Newton or Chandra (Koutroumpa et al. 2007; Henley & Shelton 2008). The results are generally consistent with a view that the Suzaku intensities are lower than XMM-Newton and Chandra, which is interpreted to be due to difference in solar wind activity. However, as shown in Figure 5, the ROSAT R45-band intensities estimated from Suzaku best-fit spectral parameters are consistent with the ROSAT All Sky Survey intensities even though RASS observations were performed during solar maximum. I consider that we need to carefully examine the contribution of short-term (< 1days) variable contribution in XMM-Newton and Chandra as we did for Suzaku before we compare the intensities obtained from the three missions.

References

Cox, D.P. 1998, Lecture Notes in Physics (Berling: Springer Verlag), 506, 121
Cravens, T.E.. 2000, ApJ, 532, L153
Cravens, T.E.. 2000, Robertson, I.P., & Snowden, S.L. J. Geophys. Res., 106, 24883
Ferrière, K.M. 2001, Rev. of Mod. Phys., 73, 1031
Fujimoto,R. et al. 2007, PASJ, 59, S133
Galeazzi, M. et al. 2007, ApJ, 658, 1081
Hagihara, T. et. al 2009, in proceedings of "the Energetic Cosmos: from Suzaku to Astro-H", in Otaru, Japan
Henley, D.B. et al. 2007, ApJ, 661, 304
Henley, D.B. & Shelton, R.L. 2008, ApJ, 676, 335
Kereš, D. et al. 2005, MNRAS, 363, 2
Koutroumpa, D. et al. 2006, A&A, 460, 289
Koutroumpa, D. et al. 2007, A&A, 475, 901
Koyama et al. 2007, PASJ, 59, S23
Kuntz, K.D. & Snowden, S.L. 2000, ApJ, 543, 195
Kuntz, K.D. & Snowden, S.L. 2008, ApJ, 674, 209
Lallement, R. 2004, A&A, 418, 143
Masui, K. et al. 2009, PASJ, 61, S115
McCammon, D. & Sanders, W. 1990, ARA&A, 28, 657
McCammon, D. et al. 2002, ApJ, 578, 188
Mitsuda, K. et al. 2007, PASJ, 59, S1
Mitsuda, K. et al. 2008, Prog. of Theor. Phys. Suppl, 169, 79
Serlemitsos, P.J. et al. 2007, PASJ, 59, S9
Smith, R.K. et al. 2007, PASJ, 59, S141
Snowden, S. L. et al. 1997, ApJ, 485, 125
Strickland, D.K. et al. 2004, ApJS, 151, 193
Sutherland, R.S. & Dopita, M.A. 1993, ApJS, 88, 253
Tawa et al. 2008, PASJ, 60, S11
Tüllman et al. 2006, A&A, 448, 43
Tsyganenko, N.A. & Sitnov M.I. 2005, J. Geophys. Res., 110, A03208
Yao,Y. et al. 2009, ApJ, 690, 143
Yamasaki N.Y. et al. 2009, PASJ, 61, S291
Yoshino, T. et al. 2009, PASJ, 61, 805